ISSN 0020-1685, Inorganic Materials, 2020, Vol. 56, No. 11, pp. 1138–1146. © Pleiades Publishing, Ltd., 2020.
Russian Text © The Author(s), 2020, published in Neorganicheskie Materialy, 2020, Vol. 56, No. 11, pp. 1199–1207.

Oxygen Chemisorption on the Surface of an In_2O_3 (011) Nanocrystal

K. S. Kurmangaleev[a, *], T. Yu. Mikhailova[b], and L. I. Trakhtenberg[a, c]

[a] *Semenov Federal Research Center for Chemical Physics, Russian Academy of Sciences, Moscow, 119991 Russia*
[b] *Kurnakov Institute of General and Inorganic Chemistry, Russian Academy of Sciences, Moscow, 119991 Russia*
[c] *Moscow State University, Moscow, 119991 Russia*
**e-mail: f7033@mail.ru*

Received May 8, 2020; revised June 22, 2020; accepted June 25, 2020

Abstract—Density-functional calculations are used to study the structural and electronic properties of stoichiometric and imperfect In_2O_3 (011) surfaces. We calculate energies of formation of neutral oxygen vacancies on the surface of an indium oxide nanocrystal and analyze the adsorption of an oxygen atom in its ground (triplet) state on a model imperfect surface having O_4 vacancies in different charge states. The results indicate that adsorption on a V_O^{2+} vacancy is the most energetically favorable and that the oxygen atom involved switches from a triplet state to a singlet one. We consider oxygen molecule adsorption from different initial geometric configurations on neutral O_{1-6} vacancies.

Keywords: indium oxide, chemisorption, density functional theory, oxygen, oxygen vacancies, nanocrystal
DOI: 10.1134/S0020168520110060

INTRODUCTION

Indium oxide-based nanomaterials have a rather wide application area: solar cells [1], conductometric sensors [2, 3], and optoelectronics [4]. The use of materials composed of nanometer elements is known to lead to a marked increase in the role of the specific surface area. Knowledge of surface structure and chemistry is crucial for assessing the influence of these characteristics on the engineering performance of various oxides.

Adsorption of atoms and molecules, including those of oxygen, is the first step of many chemical processes. Because of this, to understand such processes it is important to assess energy characteristics of adsorption of particles on stoichiometric or imperfect surfaces. Consider the adsorption of various oxygen species on a nanostructured indium surface, which is of practical interest in many cases. According to X-ray diffraction data, indium oxide nanoparticles have a cubic (bixbyite) structure (sp. gr. $Ia\bar{3}$, no. 206) [5]. This structure comprises indium atoms in two inequivalent Wyckoff positions, 8*b* (1/4, 1/4, 1/4) and 24*d* (*u*, 0, 1/4), and oxygen atoms in one Wyckoff position, 48*e* (*x*, *y*, *z*). In accordance with the symmetry elements of space group $Ia\bar{3}$, there are 80 atoms per unit cell [6]. Simple sections through this structure give a variety of crystallographic planes, which bound grains [7, 8]. These planes have a particular concentration and configuration of surface atoms, and each of them is characterized by its own features, related to its electronic structure, catalytic properties, and adsorption behavior.

According to surface energy calculations [9], the thermodynamic stability of crystallographic planes of indium oxide decreases in the following sequence: (111) > (011) > (211) > (001). A similar sequence, (111) > (110) > (100), was obtained by density functional calculations for other crystallographic planes of cubic indium oxide [10].

As shown in a first-principles quantum-chemical study of the adsorption of oxygen molecules on the In_2O_3 (100) surface [11] (which terminates with either a plane made up of only oxygen atoms (oxygen face) or a plane made up of only indium atoms (metallic face)), the chemisorption of oxygen molecules causes no significant surface reconstruction. No dissociative chemisorption is observed on the metallic face. The energy of adsorption of an oxygen molecule varies in a relatively narrow range, depending on the number of molecules on the surface, to the point where the surface is completely identical to the (100) surface with an oxygen face.

According to studies of O_2 adsorption on the most thermodynamically stable surface (111), which is nonpolar and can be obtained by a simple section of a three-dimensional lattice, this surface is chemically nonreactive with oxygen; that is, oxygen molecules do not form any stable structures with it [9]. At the same

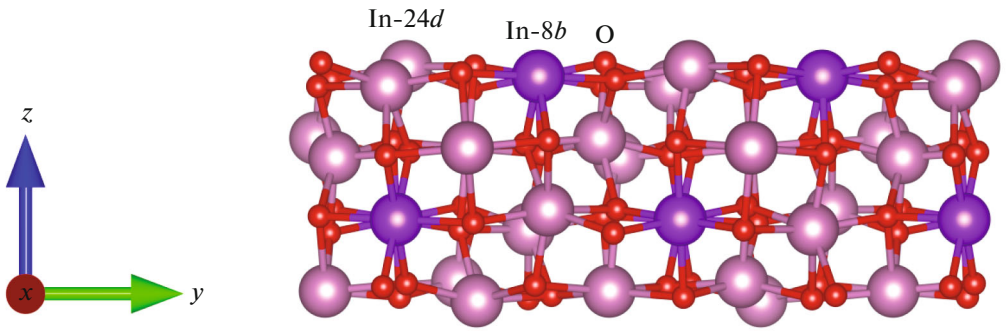

Fig. 1. (011) crystallographic plane of indium oxide.

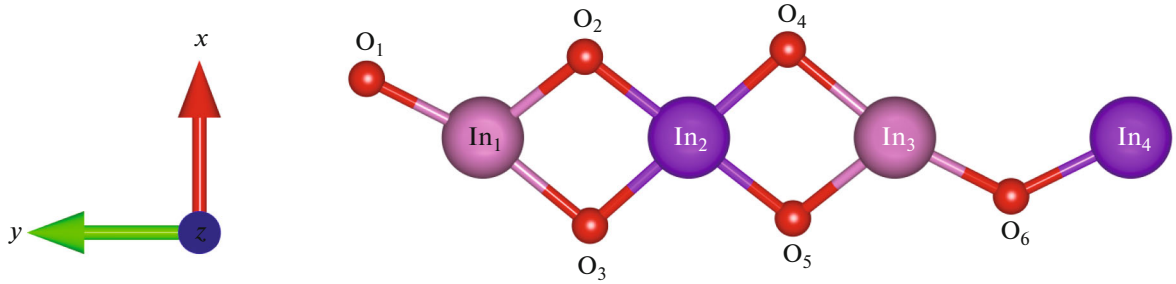

Fig. 2. Elementary repeat chain in the In_2O_3 (011)-*b* top layer.

time, adsorption on a surface oxygen vacancy leads to release of an energy on the order of 2.37 eV, and the molecule forms an adsorbate in the form of O_2^{2-} [12].

A feature common to all previous studies of the surface of transparent conductive oxides is that they dealt the adsorption of an oxygen molecule on either a stoichiometric surface or a surface with a neutral vacancy. At the same time, charge states of surface vacancies, for which adsorption energies of particles can be calculated as well, are also important.

In this paper, we present simulation results for adsorption of oxygen in atomic and molecular forms on stoichiometric and imperfect (011) surfaces having oxygen vacancies in different charge states. The (011) surface was chosen by us as the subject of this study because it is one of the most stable surfaces of cubic indium oxide and because oxygen adsorption on an imperfect (011) surface has not been analyzed previously.

MODEL AND METHOD

According to Tasker's classification [13], the (011) surface of indium oxide belongs to the first type, with a stoichiometric arrangement of the anions and cations in one atomic layer. This surface can be of two types: either a plane containing only In-24*d* cations and oxygen anions or a plane in which, along with oxygen anions, both In-24*d* and In-8*b* cations are present. In what follows, they will be denoted as (011)-*d* and (011)-*b*, respectively. The distinction between them is well seen in Fig. 1.

The top layer of the In_2O_3 (011)-*b* surface is made up of chains of indium and oxygen atoms. Its elementary repeat unit is depicted in Fig. 2.

Since the periodicity of a crystal is broken on its boundary, there are obviously dangling bonds. In particular, all of the oxygen atoms in an O_{1-6} chain have three nearest neighbors in their coordination environment, whereas the coordination number of an oxygen atom in the bulk of the crystal is four. The coordination numbers of the (In_3, In_4) and (In_1, In_2) indium atoms are four and five, respectively, whereas the coordination number of an indium cation in the bulk of the crystal is six. The same refers to the (011)-*d* In_2O_3 surface (Fig. 3).

Our calculations relied on density functional theory, utilized a plane-wave basis set, and were performed using a self-consistent calculation code built into the Quantum ESPRESSO software suite [14]. The projector augmented wave (PAW) method [15] was used to describe interactions between ions and electrons. The exchange correlation energy was estimated using a PBE functional [16]. All results were obtained at 0 K. In our calculations, we used a flat

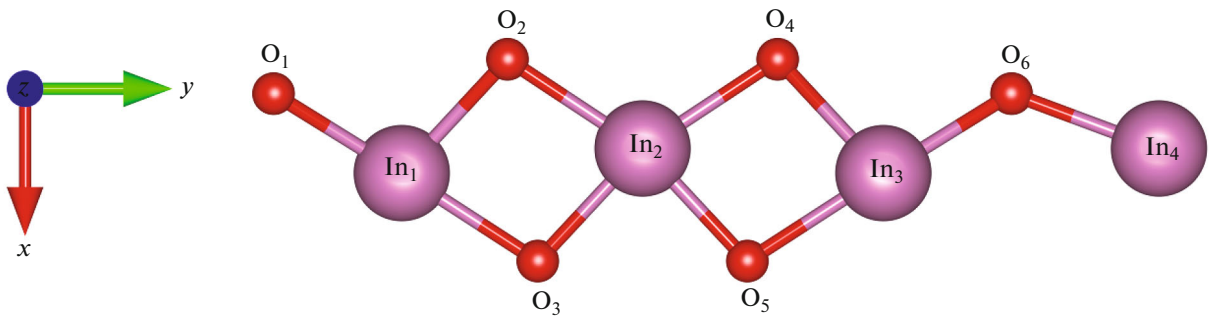

Fig. 3. Elementary repeat chain in the In_2O_3 (011)-*d* top layer.

plate model, which is obviously applicable in examining the nanoparticle surface. The choice of the model is justified by the rather small size of adsorbed particles compared to the nanoparticle size (d ~ 30–50 nm). Since the surface curvature of a large nanoparticle is relatively small, the region where the reaction takes place can be thought of as flat.

The In_2O_3 (011) surface is modeled as a flat plate 10.1171 × 14.3077 × 25.9428 Å^3 in volume, consisting of 32 indium cations and 48 oxygen anions, which form four alternating layers. It is subject to periodic boundary conditions with a vacuum gap on the order of 12 Å normal to this surface, in order to prevent effective interaction between periodic images.

The plane wave cutoff energy, determining the size of the plane-wave basis set used to expand the pseudo wave function, was 680 eV. In all our calculations, we used a k-grid [17] and chose a planar 6 × 6 × 1 grid. In all optimization processes, that is, in minimizing the energy of the system, we used the Broyden–Fletcher–Goldfarb–Shanno algorithm, built into Quantum ESPRESSO, until the forces acting on the ions were < 0.03 eV/Å.

The standard enthalpy of formation of indium oxide is

$$\Delta H_f^0(In_2O_3) = \mu_{In_2O_3}^{bulk} - 2\mu_{In}^{In\,met} - 3\mu_O^{O_2}, \quad (1)$$

where $\mu_{In}^{In\,met}$ is the chemical potential of indium (which has a tetragonal crystal structure, sp. gr. $I4/mmm$ [18]) in its standard state before the preparation of indium oxide, and $\mu_O^{O_2}$ is the chemical potential of oxygen gas under standard conditions.

The chemical potential of bulk indium oxide is constant at

$$\mu_{In_2O_3}^{bulk} = 2\mu_{In}^{In_2O_3} + 3\mu_O^{In_2O_3}. \quad (2)$$

Further, we introduce two variables for the corresponding chemical elements relative to their standard states:

$$\Delta\mu_{In} = \mu_{In}^{In_2O_3} - \mu_{In}^{In\,met}, \quad (3)$$

$$\Delta\mu_O = \mu_O^{In_2O_3} - \mu_O^{O_2}. \quad (4)$$

It is worth noting that the quantities $\Delta\mu_{In}$ and $\Delta\mu_O$ should be negative; otherwise, crystalline indium oxide would decompose into its constituent components. The enthalpy of formation of In_2O_3 has the following form:

$$\Delta H_f^0(In_2O_3) = 2\Delta\mu_{In} + 3\Delta\mu_O. \quad (5)$$

This yields the accessible range for the chemical potentials $\Delta\mu_{In}$ and $\Delta\mu_O$:

$$\frac{1}{2}\Delta H_f^0(In_2O_3) < \Delta\mu_{In} < 0, \quad (6)$$

$$\frac{1}{3}\Delta H_f^0(In_2O_3) < \Delta\mu_O < 0. \quad (7)$$

The calculated enthalpy of formation of indium oxide, $\Delta H_f^0(In_2O_3) = 10.93$ eV, approaches the experimental value reported by Cordfunke et al. [19]: 9.58 eV [19].

The probability of vacancy formation can be expressed through the vacancy formation energy. In the case of a neutral vacancy, it is given by

$$E^f = E_{slab}(V_O) - E_{slab}(In_2O_3) + \mu_O^{In_2O_3}, \quad (8)$$

where $E_{slab}(V_O)$ is the calculated total energy of a plate containing a V_O neutral vacancy, and $E_{slab}(In_2O_3)$ is the total energy of the vacancy-free plate. However, $\mu_O^{In_2O_3} = \Delta\mu_O + \mu_O^{O_2} = \Delta\mu_O + \frac{1}{2}E_{O_2}$, where E_{O_2} is the total energy of a molecule calculated by the density functional method. In what follows, the vacancy energy is analyzed under the assumption that $\Delta\mu_O = 0$.

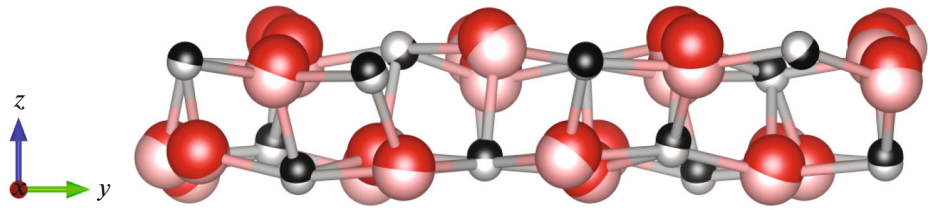

Fig. 4. Relative positions of the indium cations and oxygens in the two top layers of the (011) plate before (light circles) and after (dark circles) relaxation. The larger circles represent oxygens, and the smaller circles represent indium atoms.

The surface on which adsorption processes take place is called an adsorbent. Adsorbate is any particle (molecule or atom) adsorbed on this surface. The adsorption energy is given by

$$E_{ads} = E_{\frac{slab}{adsorbate}} - (E_{slab} + E_{adsorbate}), \quad (9)$$

where $E_{slab/adsorbate}$ is the total energy of the plate and the particle adsorbed on it, E_{slab} is the total energy of the plate, and the last term represents the total energy of the adsorbate. Thus, if the energy E_{ads} is negative, adsorption on the surface leads to the formation of a stable structure and the process is exothermic, otherwise the process is endothermic. In simulating molecular adsorption (with a normal and a parallel O_2 orientation relative to the surface), we assume the main triplet state $^3\Sigma_g^-$ and the equilibrium bond length $r_{O-O} \approx 1.21$ Å [20].

RESULTS AND DISCUSSION

We consider the effect of relaxation on surface layers of a stoichiometric plate that models the surface of an indium oxide nanocrystal and a plate having surface oxygen vacancies in different charge states, present formation energies of neutral oxygen vacancies on the surface and the energy of adsorption of an oxygen molecule normal and parallel to the surface on the vacancies, and discuss the effect of adsorption of an oxygen molecule on the density of electron states in the plate.

Atomic structure and surface relaxation. Producing a plate from a three-dimensional supercell breaks up its symmetry and introduces a vacuum region on each side of the plate. As a result, surface atoms are subjected to uncompensated forces of interatomic interaction. One way to reduce the effect of these forces is to ensure relaxation of a few surface layers of the plate being simulated, while fixing the atoms in the other layers, which will describe the configuration inside of the indium oxide.

In all our calculations, we fix two lower layers in accordance with the bulk structure of indium oxide and relax the upper layers together with the adsorbate. A plate with the (011) crystallographic plane is nonpolar: it has no sum dipole moment. Moreover, a section has no effect on the bulk stoichiometry of the crystal, so only slight atomic displacements should be observed during the relaxation of the two upper layers.

Indeed, after relaxation all of the oxygen anions are shifted in the positive direction of the z-axis. The indium cations in the second layer exhibit similar behavior (Fig. 4). The largest displacement reaches no more than 4% in comparison with the smallest size of the cell in which the plate is considered.

Formation energy of surface oxygen vacancies. Consider an In_2O_3-type lattice made up of metallic ions with a charge of 3+ and metalloid ions with a charge of 2–. The In^{3+} and O^{2-} ions have a closed electron shell with zero valence. Removing a neutral oxygen atom from the surface of an ideal indium oxide lattice produces a neutral oxygen vacancy, V_O^0, that is, an empty oxygen site, with two electrons localized near it. In a similar manner, removing oxygen anions, one can obtain charged vacancies in the In_2O_3 crystal lattice: V_O^+ and V_O^{2+}. Here, we consider the In_2O_3 (011)-b surface from which in accordance with the above procedure an oxygen atom is removed from the O_4 site (Fig. 2). Judging from the supercell size, the defect density is 2.66×10^{20} cm^{-3}.

After the relaxation of the model with a neutral vacancy, the following picture is observed: The cations around the vacancy pull away from the vacancy localization site by no more than 2.7% relative to the smallest characteristic size of the cell in which the plate is considered. At the same time, the oxygen anions approach the neutral vacancy by no more than 3.1%. A similar situation occurs for charged oxygen vacancies. Indeed, in the case of a singly charged oxygen vacancy, V_O^+, the displacement of the oxygen anions is 3.4% and that of the indium cations is 2.8%. In the case of a V_O^{2+} vacancy, the displacement of the oxygen anions far exceeds that in the above cases, reaching 3.6%, and the displacement of the indium cations is 3.7%.

The calculated total energies of the stoichiometric plate and the relaxed plate containing various neutral defects and the chemical potential of oxygen allowed us to evaluate the probability of vacancy formation using relation (1). Neutral defects were generated by sequentially removing oxygens from positions O_{1-6} (Fig. 2). The corresponding data are presented in Table 1. It is seen that the formation of an O_4 vacancy has the highest probability.

Oxygen molecule adsorption on a stoichiometric surface. Theoretical studies suggest that, in the case of adsorption of an oxygen atom or molecule, there are no stable structures of a stoichiometric surface with these species on the (111) surface or the surface under consideration, (011) [9].

Oxygen atom and molecule adsorption on an imperfect surface. Since an O_4 oxygen vacancy is the most likely to be formed, consider oxygen atom adsorption precisely on this vacancy in different charge states and oxygen molecule adsorption on all types of O_{1-6} neutral vacancies (Fig. 2). The corresponding molecule or atom was placed a distance on the order of 2 Å over the surface and then the plate–atom (molecule) system was optimized at constant positions of the atoms in the two lower layers.

Since adsorption can be accompanied by molecule dissociation, calculations should take into account spin polarization as well, because dissociation products can have a nonzero net spin. One should also take into account spin polarization in atoms and molecules with unpaired electrons, in particular in the case of an oxygen atom and molecule in their ground (triplet) state.

The presence of a surface defect is favorable for the adsorption of both atomic and molecular oxygen. We examined three types of O_4 vacancies differing in charge state. The energy of oxygen atom adsorption on an oxygen vacancy is given in Table 2.

The observed decrease in the energy of oxygen atom adsorption with an increase in the charge on an O_4 oxygen vacancy can be accounted for by the fact that a neutral vacancy on the crystal surface forms two local free valences, which will never meet by virtue of Coulomb repulsion. An adsorbed oxygen atom will then form a strong bond with the neutral vacancy, incorporating itself into the crystal lattice, as confirmed by the present adsorption energy calculations and the zero total magnetization. Since a V_O^+ vacancy has one local surface free valence, the formation of a bond with an oxygen atom will leave one unpaired electron in one of its *p*-orbitals. Because of this, according to calculations the total magnetization is approximately unity: $0.9\mu_B$ per unit cell. In the case of a V_O^{2+} vacancy, the energy released upon adsorption is

Table 1. Energy of oxygen vacancy formation on the indium oxide (011) surface

V_O vacancy	O_1	O_2	O_3	O_4	O_5	O_6
Formation energy, eV	8.42	7.77	7.77	5.37	8.62	8.59

Table 2. Data on the energy of oxygen atom adsorption on O_4 vacancies in different charge states and the total magnetic moment per unit cell

Charge state of a vacancy	E_{ads}^{O}, eV	M_{total}, μ_B
0	–5.364	0.00
1+	–4.738	0.90
2+	–5.851	0.00

(011)-*b* surface.

–5.851 eV, and an atom that fills the oxygen vacancy switches from a triplet state to a singlet one.

Calculations of the energy of oxygen molecule adsorption on neutral vacancies indicates that the initial geometry of the location of an oxygen molecule (Fig. 5) with respect to the indium oxide surface has a significant effect. The corresponding data are presented in Table 3.

Clearly, adsorption of an oxygen atom and molecule on a neutral vacancy leads to an electron density redistribution from the indium oxide plate to the oxygen species. This is evidenced by the changes in the Löwdin charges [21] on adsorbate atoms, as well as by changes in the interatomic distance in the adsorbed oxygen molecule, which varies from 1.332 to 1.496 Å on different oxygen vacancies. This points to a tendency toward the formation of O_2^- and O_2^{2-} ionic oxygen species, with an interatomic distance on the order of 1.33 and 1.49 Å, respectively [22]. Therefore, during the adsorption process the plate acts as an electron donor and an oxygen molecule acts as an acceptor, reducing the surface conductivity of the plate.

Also presented in Table 3 are the total magnetic moments per unit cell (the magnetic moment of a free oxygen atom and molecule is $2\mu_B$).

The band gap determined by density functional calculations in the generalized gradient approximation (GGA) or local-density approximation (LDA) is known to be underrated. Indeed, the fundamental band gap calculated by us for a plate consisting of four atomic layers and subject to periodic boundary conditions along all three coordinate axes is 1.18 eV against the experimentally determined 2.7 eV [23].

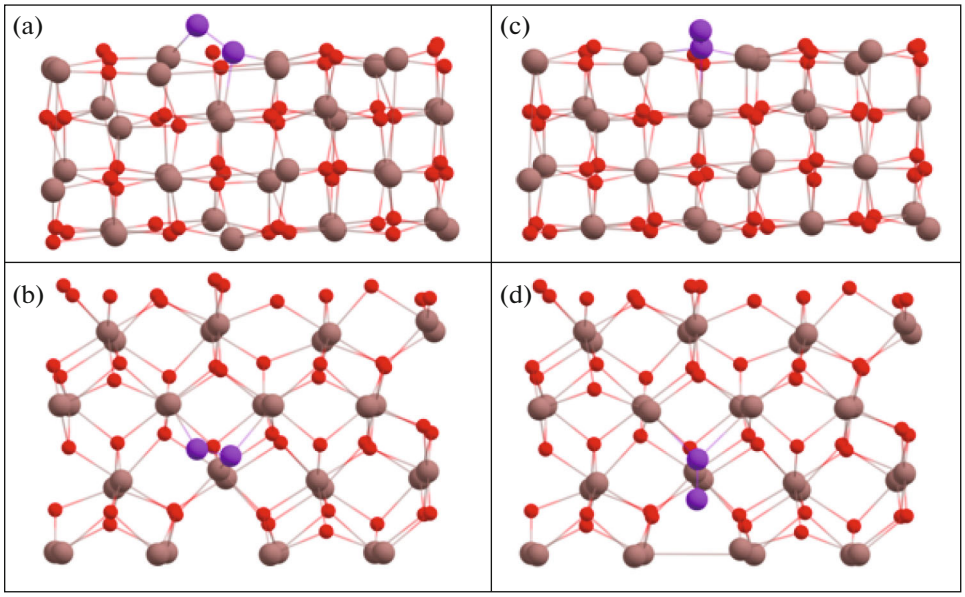

Fig. 5. Configuration of an oxygen molecule on a neutral vacancy after adsorption in relation to the initial geometry relative to the surface: (a, b) molecule parallel to the surface over an O_4 vacancy before optimization (side and top views, respectively); (c, d) molecule that was normal to the surface before optimization (in both cases, the molecules were located 2 Å from the topmost surface atom).

Density of electron states. Clearly, a significant contribution to the valence band top is made by the *p*- and *s*-orbitals of the indium atoms located on the surface of the plate and having three nearest neighbors in their coordination environment. In particular, mixing of these orbitals is possible. It is worth noting that partial densities of the indium *d*-orbitals contribute to the total electron density of low-lying bands in the range −15.6 and −13.0 eV. The region of the peaks at −20.18 and −17.6 eV is characterized by possible hybridization of the *s*- and *p*-orbitals of indium atoms and the *s*-orbitals of the oxygen atoms in the crystal lattice (Figs. 6a, 6b). In Fig. 7a, one can see small additional peaks in comparison with the total density of electron states in the plate with a neutral O_4 vacancy (Fig. 7b) as a result of the participation of the *s*- and *p*-orbitals of the oxygen atoms of a molecule adsorbed from a position normal to the plane of the plate and located over a neutral O_4 vacancy (Figs. 6c, 6d). Moreover, adsorption causes the line spectrum of densities of the *p*-orbitals of an oxygen atom in a free molecule (Figs. 6e, 6f) to transform into a continuous spectrum, which contributes to both the valence band and a region near the bottom of the conduction band of the material.

Table 3. Energy of oxygen molecule adsorption (E_{ads}) on V_O neutral vacancies, interatomic distance in the adsorbed molecule ($r_{O–O}$), total magnetic moment per unit cell (M_{total}), and Löwdin charges (q) on the atoms of the adsorbed oxygen molecule

V_O	E_{ads}, eV	$r_{O–O}$, Å	M_{total}, μ_B	q		E_{ads}, eV	$r_{O–O}$, Å	M_{total}, μ_B	q	
	horizontal					vertical				
O_1	−1.613	1.477	−0.03	−0.364	−0.364	−0.855	1.362	0.81	−0.221	−0.213
O_2	−0.910	1.338	0.96	−0.180	−0.171	−0.522	1.332	1.01	−0.206	−0.162
O_3	−0.899	1.462	0.13	−0.372	−0.359	−0.929	1.485	0.07	−0.373	−0.391
O_4	−1.657	1.477	0.08	−0.383	−0.374	−1.054	1.472	−0.14	−0.344	−0.376
O_5	−1.526	1.485	0.00	−0.384	−0.363	−1.485	1.485	0.00	−0.379	−0.383
O_6	−1.755	1.496	0.00	−0.385	−0.352	−0.796	1.377	0.75	−0.237	−0.236

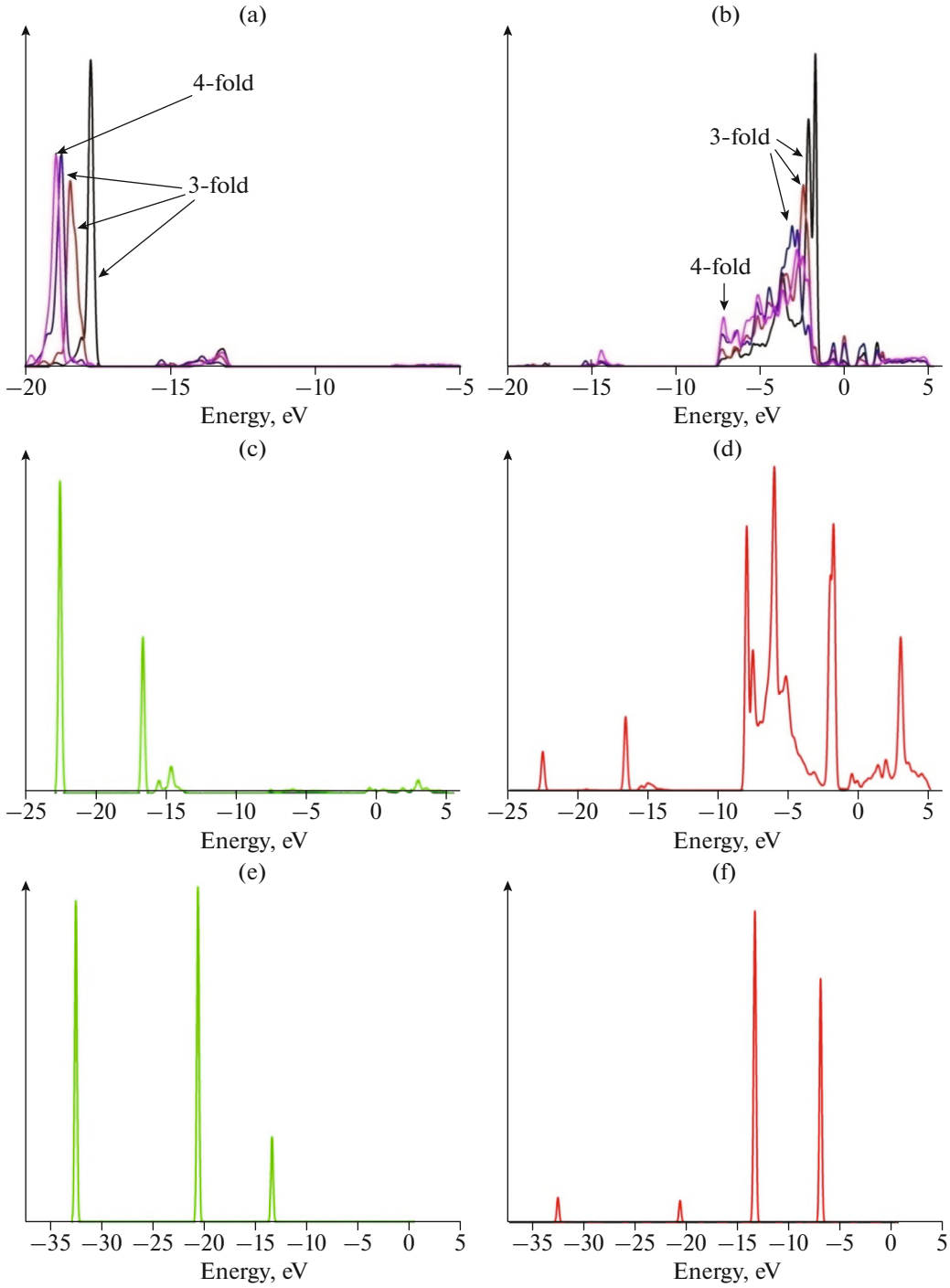

Fig. 6. Partial density of electron states: (a, b) contributions of the *s*- and *p*-orbitals of oxygen atoms with different coordination numbers to the density of states in a stoichiometric plate, respectively; (c, d) partial electron densities of the *s*- and *p*-orbitals of an atom incorporated into a plate upon adsorption of an oxygen molecule on a neutral O_4 vacancy; (e, f) partial electron densities of the *s*- and *p*-orbitals of an atom in a free oxygen molecule, respectively.

CONCLUSIONS

Using density-functional calculations, we have studied the structural and electronic properties of both a stoichiometric and an imperfect In_2O_3 (011) surface. We have calculated energies of formation of oxygen vacancies, which indicate that the formation of O_4 vacancies is the most probable. Analysis of the adsorption of an oxygen atom in its ground (triplet) state on O_4 vacancies in different charge states shows that the highest energy is released in the case of adsorption on

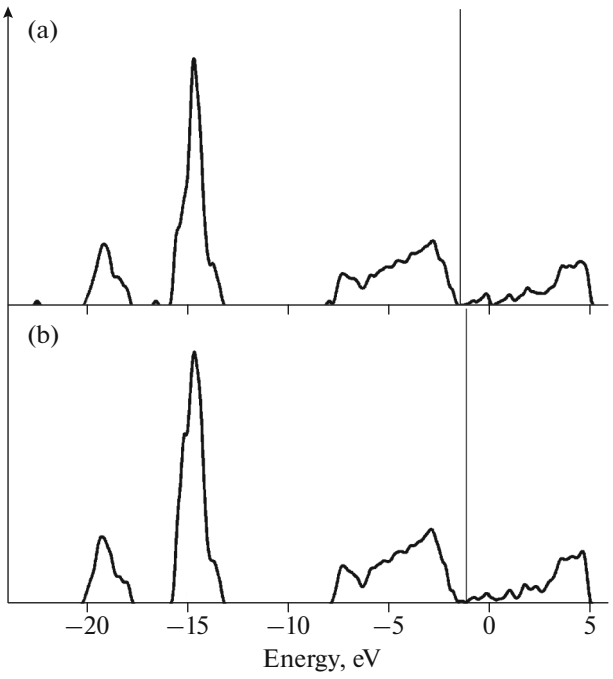

Fig. 7. Total density of electron states: (a) total density of states in a plate with an adsorbed oxygen molecule which was first oriented vertically and locates over an O_4 vacancy; (b) total density of states with a neutral O_4 vacancy (the vertical line shows the Fermi energy).

a V_O^{2+} vacancy and that the atom that fills the oxygen vacancy switches from a triplet state to a singlet one.

We have considered a number of cases with oxygen molecule adsorption from different geometric configurations relative to the plane of the plate on neutral $O_{1–6}$ vacancies. The internuclear distance in oxygen molecules adsorbed on various oxygen vacancies ranges from 1.332 to 1.496 Å, pointing to a tendency toward the formation of O_2^- and O_2^{2-} ionic oxygen species. We are thus led to conclude that, during the adsorption process, the plate acts as an electron donor and the oxygen molecule acts as an electron acceptor, reducing the surface conductivity of the plate. The increased internuclear distance in adsorbed oxygen molecules points to a tendency toward dissociative chemisorption.

FUNDING

This work was supported by the Russian Federation Ministry of Science and Higher Education (state research target no. 0082-2018-0003 for the Semenov Federal Research Center for Chemical Physics, Russian Academy of Sciences, theme no. 45.22: Fundamental Principles behind the Development of a New Generation of Nanostructured Systems with Unique Performance Parameters, state registration no. AAAA-A18-118012390045-2) and the Russian Foundation for Basic Research (grant nos. 19-37-90016 and 19-07-00141a).

ACKNOWLEDGMENTS

We are grateful to our colleagues at the Joint Supercomputer Center, Russian Academy of Sciences, for providing us with necessary computational resources.

REFERENCES

1. Chen, P., Yin, X., Que, M., Liu, X., and Que, W., Low temperature solution processed indium oxide thin films with reliable photoelectrochemical stability for efficient and stable planar perovskite solar cells, *J. Mater. Chem. A,* 2017, vol. 5, pp. 9641–9648.
2. Baratto, C., Ferroni, M., Faglia, G., and Sberveglieri, G., Iron-doped indium oxide by modified RGTO deposition for ozone sensing, *Sens. Actuators, B,* 2006, vol. 118, nos. 1–2, pp. 221–225.
3. Yamaura, H., Jinkawa, T., Tamaki, J., Moriya, K., Miura, N., and Yamazoe, N., Indium oxide based gas sensor for selective detection of CO, *Sens. Actuators, B,* 1996, vol. 36, nos. 1–3, pp. 325–332.
4. Golan, G., Axelevitch, A., Gorenstein, B., and Peled, A., Novel type of indium oxide thin films sputtering for opto-electronic applications, *Appl. Surf. Sci.,* 2007, vol. 253, no. 15, pp. 6608–6611.
5. Fang, Z., Assaaoudi, H., Guthrie, R.I.L., Kozinski, J.A., and Butler, I.S., Continuous synthesis of tin and indium oxide nanoparticles in sub- and supercritical water, *J. Am. Ceram. Soc.,* 2007, vol. 90, no. 8, pp. 2367–2371.
6. Marezio, M., Refinement of the crystal structure of In_2O_3 at two wavelengths, *Acta Crystallogr.,* 1966, vol. 20, no. 6, pp. 723–728.
7. Hao, Y., Meng, G., Ye, C., and Zhang, L., Controlled synthesis of In_2O_3 octahedrons and nanowires, *Cryst. Growth Des.,* 2005, vol. 5, no. 4, pp. 1617–1621.
8. Shi, M., Xu, F., Yu, K., Zhu, Z., and Fang, J., Controllable synthesis of In_2O_3 nanocubes, truncated nanocubes, and symmetric multipods, *J. Phys. Chem. C,* 2007, vol. 111, no. 44, pp. 16267–16271.
9. Agoston, P. and Albe, K., Thermodynamic stability, stoichiometry, and electronic structure of bcc-In_2O_3 surfaces, *Phys. Rev. B:, Condens. Matter Mater. Phys.,* 2011, vol. 84, paper 045311.
10. Walsh, A. and Catlow, C.R.A., Structure, stability and work functions of the low index surfaces of pure indium oxide and Sn-doped indium oxide (ITO) from density functional theory, *J. Mater. Chem.,* 2010, vol. 20, no. 46, pp. 10438–10444.
11. Zhou, C., Li, J., Chen, S., Wu, J., Heier, K.R., and Cheng, H., First-principles study on water and oxygen adsorption on surfaces of indium oxide and indium tin oxide nanoparticles, *J. Phys. Chem. C,* 2008, vol. 112, no. 36, pp. 14015–14020.
12. Inerbaev, T., Sahara, R., Mizuseki, H., Kawazoe, Y., and Nakamura, T., Theoretical modeling of oxygen and water adsorption on indium oxide (111) surface, *ACS Symp. Ser.,* 2015, vol. 1196, pp. 137–149.

13. Tasker, P.W., The stability of ionic crystal surfaces, *J. Phys. C: Solid State Phys.,* 1979, vol. 12, no. 22, pp. 4977–4984.

14. Giannozzi, P., Baroni, S., Bonini, N., Calandra, M., Car, R., Cavazzoni, C., Ceresoli, D., Chiarotti, G.L., Cococcioni, M., Dabo, I., Dal Corso, A., Fabris, S., Fratesi, G., de Gironcoli, S., Gebauer, R., Gerstmann, U., Gougoussis, C., Kokalj, A., Lazzeri, M., Martin-Samos, L., Marzari, N., Mauri, F., Mazzarello, R., Paolini, S., Pasquarello, A., Paulatto, L., Sbraccia, C., Scandolo, S., Sclauzero, G., Seitsonen, A.P., Smogunov, A., Umari, P., and Wentzcovitch, R.M., A modular and open-source software project for quantum simulations of materials, *J. Phys.: Condens. Matter,* 2009, vol. 21, paper 395502. http://arxiv.org/abs/0906.2569

15. Kresse, G. and Joubert, D., From ultrasoft pseudopotentials to the projector augmented-wave method, *Phys. Rev. B: Condens. Matter Mater. Phys.,* 1999, vol. 59, pp. 1758–1775.

16. Perdew, P., Burke, K., and Ernzerhof, M., Generalized gradient approximation made simple, *Phys. Rev. Lett.,* 1996, vol. 77, pp. 3865–3868.

17. Monkhorst, H.J. and Pack, J.D., Special points for Brillouin-zone integrations, *Phys. Rev. B: Solid State,* 1976, vol. 13, pp. 5188–5192.

18. Smith, J.F. and Schneider, V.L., Anisotropic thermal expansion of indium, *J. Less-Common Met.,* 1964, vol. 7, no. 1, pp. 17–22.

19. Cordfunke, E.H.P., Konings, R.J.M., and Ouweltjes, W., The standard enthalpy of formation of In_2O_3, *J. Chem. Thermodyn.,* 1991, vol. 23, no. 5, pp. 451–454.

20. Huber, K.P. and Herzberg, G., *Molecular Spectra and Molecular Structure,* New York: Van Nostrand, 1979, vol. 4.

21. Löwdin, P.O., On the non-orthogonality problem, *Adv. Quantum Chem.,* 1970, vol. 5, pp. 185–199.

22. Che, M. and Tench, A.J., Characterization and reactivity of molecular-oxygen species on oxide surfaces, *Adv. Catal.,* 1983, vol. 32, pp. 1–148.

23. Bourlange, A., Payne, D.J., Egdell, R.G., Foord, J.S., Edwards, P.P., Jones, M.O., Schertel, A., Dobson, P.J., and Hutchison, J.L., Growth of In_2O_3(100) on Y-stabilized ZrO_2(100) by O-plasma assisted molecular beam epitaxy, *Appl. Phys. Lett.,* 2008, vol. 92, no. 9, pp. 092117–092120.

Translated by O. Tsarev